16th World Conference on Earthquake, 16WCEE 2017

Santiago Chile, January 9th to 13th 2017

Paper N° 1117

Registration Code: S-0000013262

OPTIMIZATION OF BUCKLING RESTRAINED BRACED FRAME UNDER SEISMIC LOADING

J. Xu[(1)], G. Fermandois-Cornejo[(2)], B.F. Spencer Jr. [(3)], X. Lu[(4)]

[(1)] *Doctoral Candidate, State Key Laboratory of Disaster Reduction in Civil Engineering, Tongji Univ., Shanghai 200092, China. jiaqixu@illinois.edu*
[(2)] *Doctoral Candidate, Dept. of Civil and Environmental Engineering, Univ. of Illinois, Urbana, IL 61801, fermand2@illinois.edu*
[(3)] *Newmark Endowed Chair of Civil Engineering, Univ. of Illinois, Urbana, IL 61801, bfs@illinois.edu*
[(4)] *Professor, State Key Laboratory of Disaster Reduction in Civil Engineering, Tongji Univ., Shanghai 200092, China. lxlst@tongji.edu.cn*

Abstract

This study proposes a design procedure for the optimization of buckling restrained braced frames (BRBF) subjected to seismic loading. The stiffness distribution of the buckling restrained braces (BRBs) is optimized at the system-level. The parameters of a BRB component can be obtained according to the optimized stiffness. The seismic excitation is represented as a zero-mean filtered white noise and is formulated in the augmented state space with the BRBF structure. The hysteretic behavior of the BRB components are represented by the Bouc-Wen model and linearized to fit the state space formulation. The optimization objective is defined in terms of stationary structural responses. In the illustrative example, ductility and interstory drift are considered as the optimization objectives. The optimized results are compared with the common design practice according to the equivalent lateral force (ELF) procedure as specified by ASCE-7. The optimal BRBF design with minimized interstory drift response is similar to the design obtained by the ELF procedure, which, however, usually results in soft stories and nonuniform energy dissipation along the height. To uniformly distribute and minimize the ductility demand of the BRBF, the optimized design tends to distribute the stiffness inversely proportional with height and more stiffness is distributed at the first floor.

Keywords: Structural optimization; buckling restrained braced frame; seismic response, stochastic loading

1. Introduction

The ability to dissipate energy is an essential feature of a structural design subjected to high-intensity earthquakes. Since Skinner et al. [1] employed yielding metallic devices to reduce seismic responses of frame structures, buckling restrained braces (BRBs) have become one of the most frequently applied energy dissipating devices. BRBs have been broadly accepted in Japan since the 1995 Kobe earthquake and soon after the 1994 Northridge earthquake in the U.S.A. Currently, buildings in Taiwan are commonly constructed with BRBs as the primary lateral resisting system [2]. The BRB system is widely utilized in residential buildings and other civil infrastructure during the last few decades, both in new-constructions and retrofitted-structures [3].

The buckling restrained braced frame (BRBF) has superior energy dissipating capability compared with steel frame with conventional braces. During high-intensity earthquake, the basic structural framework of the BRBF remains linearly elastic, and the BRBs dissipate seismically-induced energy by yielding. BRBs can fully yield in both tension and compression without buckling, which results in symmetric hysteresis loops [4] and stable energy dissipation [5]. A considerable amount of literature has been published on the research of BRBF, both analytically [6] and experimentally [5, 7]. Conventional BRBs are designed based on the equivalent lateral force (ELF) method as recommended by ASCE-7, which cannot guarantee an optimized design with uniform energy dissipation [7]. While under-dimensioned BRBs are not able to provide enough seismic capacity, over-dimensioned BRBs will remain elastic during high-intensity earthquakes. The energy dissipation of BRBF with over-dimensioned BRBs will concentrate in soft floors, which is dangerous for the floors with insufficient post-yielding lateral stiffness. Therefore, designing BRBF with structural optimization is of great significance.

Earthquake ground motions are random in nature and frequently modeled as random processes [8]. As a result, structural optimization of a BRBF is a stochastic optimization problem. To represent the seismic loading and associated structural responses, several studies have employed Monte Carlo simulation (MCS) in the optimization procedure (e.g., [7]). Although such time history analysis can capture important structural behaviors, it can be computationally expensive. When implemented in a structural optimization procedure, which requires numerous MCS analyses at each iteration step, the resulting scheme can be prohibitively time consuming and computationally demanding. Furthermore, each simulation merely represents realizations of individual earthquakes, hence obtaining converged statistical results can be challenging.

This study proposes a stochastic structural optimization procedure for BRBF subjected to high-intensity seismic excitation. The procedure optimizes the stiffness distribution of the BRBs at the system-level. Subsequently, the parameters of a specific BRB component is designed according to the obtained optimal stiffness at the component-level. The proposed approach incorporates the stochastic nature of the seismic loading directly in the optimization procedure. Equivalent linearization is employed, along with random vibration theory, to determine the stationary structural responses and construct the objective function in the optimization procedure. An example is presented to illustrate the proposed approach in which the random input is modeled by the Kanai-Tajimi (KT) spectrum. The hysteretic behavior of the BRBs is represented by the Bouc-Wen model. The exampled BRBF optimization results demonstrate the efficacy of the proposed approach. The difference between the BRB designs minimizing interstory drift and ductility are also discussed in this paper.

2. Problem formulation

This section describes the formulation of the proposed BRBF optimization procedure. A typical seismic ground acceleration is an inherently nonstationary stochastic process. However, if only the strong-motion content is required for peak structural response estimation, a stationary process can be a good approximation [8]. Therefore, the excitation is represented as a stationary filtered white noise in this study. The structure is characterized by the state space representation, which is a system of first-order ordinary differential equations. The hysteretic behavior of the BRB components is represented by the Bouc-Wen model. Analysis of the system is carried out via equivalent linearization. The optimization objective is defined in terms of the stationary structural responses.

2.1 Structural model description

The equation of motion (EOM) of an *N*-degree of freedom (*N*DOF) BRBF with nonlinear BRBs is given by

$$\mathbf{M}\ddot{\mathbf{u}} + \mathbf{C}\dot{\mathbf{u}} + \mathbf{K}\mathbf{u} + \mathbf{r}_{\mathrm{b}}(t) = \mathbf{G}\mathbf{p}(t) \tag{1}$$

where $\mathbf{u}$, $\dot{\mathbf{u}}$, $\ddot{\mathbf{u}}$ are the displacement, velocity and acceleration vectors, respectively. $\mathbf{M}$ is the mass matrix, $\mathbf{C}$ is the damping matrix and $\mathbf{K}$ is the stiffness matrix of the basic structural framework, which are considered as known deterministic parameters. $\mathbf{r}_{\mathrm{b}}(t)$ represents the restoring force provided by the BRBs. $\mathbf{G}$ is a matrix coupling the dimension of the excitation and the structural degrees of freedom. In this study, because the BRBs are the main elements to provide lateral stiffness, the linear elastic stiffness component $\mathbf{K}$ is neglected [7, 9]. $\mathbf{p}(t)$ is the input excitation vector and is represented as a filtered white noise as

$$\begin{aligned} \dot{\mathbf{x}}_{\mathrm{g}} &= \mathbf{A}_{\mathrm{g}}\mathbf{x}_{\mathrm{g}} + \mathbf{B}_{\mathrm{g}}\mathbf{w}(t) \\ \mathbf{p}(t) &= \mathbf{C}_{\mathrm{g}}\mathbf{x}_{\mathrm{g}} \end{aligned} \tag{2}$$

where $\mathbf{A}_{\mathrm{g}}$, $\mathbf{B}_{\mathrm{g}}$ and $\mathbf{C}_{\mathrm{g}}$ represent the characteristics of the excitation. The mean and autocorrelation of the vectored white noise $\mathbf{w}(t)$, are

$$\mathrm{E}\left[\mathbf{w}(t)\right] = 0, \quad \mathrm{E}\left[\mathbf{w}(t)\mathbf{w}^{\mathrm{T}}(t+\tau)\right] = 2\pi\mathbf{S}_0\delta(\tau) \tag{3}$$

where $\mathrm{E}[\cdot]$ is the expectation operator, $\mathbf{S}_0$ is the magnitude of the constant two-sided power spectral density matrix, and $\delta(\tau)$ is the Dirac delta function.

In this paper, the Bouc-Wen model [10, 11] is adopted to describe $\mathbf{r}_{\mathrm{b}}(t)$, the hysteretic restoring force of the BRBs,

$$\mathbf{r}_{\mathrm{b}}(t) = \alpha\mathbf{K}_{\mathrm{b}}\mathbf{u} + (1-\alpha)\mathbf{K}_{\mathrm{b}}u_{\mathrm{y}}\mathbf{z}(t) \tag{4}$$

where α is the rigidity ratio, $\mathbf{K}_{\mathrm{b}}$ is the stiffness matrix of the BRB components. u_{y} is the yielding displacement. The evolutionary variable $\mathbf{z}(t)$ models the hysteretic behavior of the restoring force. The evolutionary variable associated with the j^{th} floor, z_j, can be described by the differential equation [11],

$$\dot{z}_j = -\frac{1}{u_{\mathrm{y}}}\left(\gamma\,|\,\dot{d}_j\,|\,|\,z_j\,|^{n-1}\,z_j + \beta\dot{d}_j\,|\,z_j\,|^{n} - A\dot{d}_j\right) \tag{5}$$

where A, γ, β and n are the shape coefficients of the hysteresis loop. The parameters of the Bouc-Wen model for each BRB are assumed to be the same in this paper. d_j is the interstory drift between the consecutive j^{th} and $(j-1)^{\mathrm{th}}$ floor (i.e., $d_j = u_j - u_{j-1}$). By equivalent linearization, $\mathbf{z}(t)$ can be rewritten in the first-order state space form related with the velocity vector $\dot{\mathbf{d}}$ as

$$\dot{\mathbf{z}} + \mathbf{C}_{\mathrm{eq}}\dot{\mathbf{d}} + \mathbf{K}_{\mathrm{eq}}\mathbf{z} = \mathbf{0} \tag{6}$$

The standard statistical linearization matrices $\mathbf{C}_{\mathrm{eq}}$ and $\mathbf{K}_{\mathrm{eq}}$ are given by [12],

$$\mathbf{K}_{\mathrm{eq},ij} = \mathrm{E}\left[\frac{\partial r_i}{\partial d_j}\right], \quad \mathbf{C}_{\mathrm{eq},ij} = \mathrm{E}\left[\frac{\partial r_i}{\partial \dot{d}_j}\right] \tag{7}$$

Wen [12] evaluated the equivalent matrices $\mathbf{C}_{\text{eq}}$ and $\mathbf{K}_{\text{eq}}$ for the Bouc-Wen model assuming Gaussian excitation. With the assumption of the Gaussian excitation and the equivalent linear responses, $\dot{d}_j$ and z_j are jointly Gaussian. For $n=1$, when $i=j$,

$$\begin{aligned}\mathbf{C}_{\text{eq},ii} &= \frac{1}{u_{\text{y}}}\left(\sqrt{\frac{2}{\pi}}\left[\gamma\frac{\mathrm{E}\left(\dot{d}_i z_i\right)}{\sigma_{\dot{d}_i}}+\beta\sigma_{z_i}\right]-A\right)\\ \mathbf{K}_{\text{eq},ii} &= \frac{1}{u_{\text{y}}}\left(\sqrt{\frac{2}{\pi}}\left[\gamma\sigma_{\dot{d}_i}+\beta\frac{\mathrm{E}\left(\dot{d}_i z_i\right)}{\sigma_{z_i}}\right]\right)\end{aligned} \tag{8}$$

When $i\neq j$, $\mathbf{C}_{\text{eq},ij}=0$ and $\mathbf{K}_{\text{eq},ij}=0$. $\sigma(\cdot)$ represents the standard deviation of the subscripted variable. Expression for the more general case when $n\neq 1$ can be found in Wen [12].

Defining the state vector $\mathbf{x}_{\text{s}}$ as

$$\mathbf{x}_{\text{s}} = \left(\mathbf{u}^{\text{T}} \quad \dot{\mathbf{u}}^{\text{T}} \quad \mathbf{z}^{\text{T}}\right)^{\text{T}} \tag{9}$$

the equivalent linear structure can be cast into the state space formulation

$$\begin{aligned}\dot{\mathbf{x}}_{\text{s}} &= \mathbf{A}_{\text{s}}\mathbf{x}_{\text{s}}+\mathbf{B}_{\text{s}}\mathbf{p}\left(t\right)\\ \mathbf{y}_{\text{s}} &= \mathbf{C}_{\text{s}}\mathbf{x}_{\text{s}}+\mathbf{D}_{\text{s}}\mathbf{p}\left(t\right)\end{aligned} \tag{10}$$

where $\mathbf{y}_{\text{s}}$ is the vector of structural responses of interest; and $\mathbf{A}_{\text{s}}$ and $\mathbf{B}_{\text{s}}$ are given by,

$$\mathbf{A}_{\text{s}} = \begin{bmatrix}\mathbf{0} & \mathbf{I} & \mathbf{0}\\ -\alpha\mathbf{M}^{-1}\mathbf{K}_{\text{b}} & -\mathbf{M}^{-1}\mathbf{C} & -\left(1-\alpha\right)\mathbf{M}^{-1}\mathbf{K}_{\text{b}}\\ \mathbf{0} & -\mathbf{C}_{\text{eq}} & -\mathbf{K}_{\text{eq}}\end{bmatrix},\quad \mathbf{B}_{\text{s}} = \begin{bmatrix}\mathbf{0}\\ \mathbf{M}^{-1}\mathbf{G}\\ \mathbf{0}\end{bmatrix} \tag{11}$$

The response matrices $\mathbf{C}_{\text{s}}$ and $\mathbf{D}_{\text{s}}$ are determined depending on the specified outputs.

2.2 Stochastic model for seismic excitations

For illustrative purposes, this study uses the commonly employed spectral representation of the ground motion was proposed by Kanai [13] and Tajimi [14], i.e., the Kanai-Tajimi (KT) model; however, other representations of the ground motion is readily accommodated in the proposed approach. The seismic excitation $\mathbf{p}\left(t\right)$ modeled by the KT filter is given by

$$\begin{aligned}\ddot{z}_{\text{g}}+2\zeta_{\text{g}}\omega_{\text{g}}\dot{z}_{\text{g}}+\omega_{\text{g}}^2 z_{\text{g}} &= w\left(t\right)\\ a_{\text{g}} &= \omega_{\text{g}}^2 z_{\text{g}}+2\zeta_{\text{g}}\omega_{\text{g}}\dot{z}_{\text{g}}\end{aligned} \tag{12}$$

where a_g is the absolute ground acceleration; ω_g and ζ_g represent the site conditions; and $w\left(t\right)$ is a scalar stationary white noise process with zero mean and constant two-sided power spectra density $S_w(\omega)=S_0$. The characteristic matrices of the excitation in Eq. (2) are

$$\mathbf{A}_{\mathrm{g}} = \begin{bmatrix} 0 & 1 \\ -\omega_g^2 & -2\zeta_g\omega_g \end{bmatrix},\ \mathbf{B}_{\mathrm{g}} = \begin{bmatrix} 0 \\ 1 \end{bmatrix},\ \mathbf{C}_{\mathrm{g}} = \begin{bmatrix} \omega_g^2 & 2\zeta_g\omega_g \end{bmatrix} \tag{13}$$

An augmented state vector, $\mathbf{x}_{\mathrm{a}}$ is then defined as

$$\mathbf{x}_{\mathrm{a}} = \begin{pmatrix} \mathbf{x}_{\mathrm{s}}^{\mathrm{T}} & \mathbf{x}_{\mathrm{g}}^{\mathrm{T}} \end{pmatrix}^{\mathrm{T}} \tag{14}$$

to yield a combined representation of the structure and the excitation

$$\begin{aligned} \dot{\mathbf{x}}_{\mathrm{a}} &= \mathbf{A}_{\mathrm{a}}\mathbf{x}_{\mathrm{a}} + \mathbf{B}_{\mathrm{a}}\mathbf{w}(t) \\ \mathbf{y}_{\mathrm{s}} &= \mathbf{C}_{\mathrm{a}}\mathbf{x}_{\mathrm{a}} \end{aligned} \tag{15}$$

where

$$\mathbf{A}_{\mathrm{a}} = \begin{bmatrix} \mathbf{A}_{\mathrm{s}} & \mathbf{B}_{\mathrm{s}}\mathbf{C}_{\mathrm{g}} \\ \mathbf{0} & \mathbf{A}_{\mathrm{g}} \end{bmatrix},\ \mathbf{B}_{\mathrm{a}} = \begin{bmatrix} \mathbf{0} \\ \mathbf{B}_{\mathrm{g}} \end{bmatrix},\ \mathbf{C}_{\mathrm{a}} = \begin{bmatrix} \mathbf{C}_{\mathrm{s}} & \mathbf{D}_{\mathrm{s}}\mathbf{C}_{\mathrm{g}} \end{bmatrix} \tag{16}$$

2.3 Structural responses

The expected value of the structural responses are chosen to be the optimization objective. Assuming that the initial conditions are deterministic and known, then the initial conditions are

$$\mathbf{\Gamma}_{\mathbf{x}_{\mathrm{a}}}(0) = \mathbf{\Gamma}_0 = \mathbf{0} \tag{17}$$

Because the input in a Gaussian white noise stationary process with zero-mean, then the mean-value of structural response $\boldsymbol{\mu}_{\mathbf{x}_{\mathrm{a}}}$ is also zero. Therefore,

$$\mathbf{\Gamma}_{\mathbf{x}_{\mathrm{a}}} = \mathrm{E}\left[\left(\mathbf{x}_{\mathrm{a}} - \boldsymbol{\mu}_{\mathbf{x}_{\mathrm{a}}} \right) \left(\mathbf{x}_{\mathrm{a}} - \boldsymbol{\mu}_{\mathbf{x}_{\mathrm{a}}} \right)^{\mathrm{T}} \right] = \mathrm{E}\left[\mathbf{x}_{\mathrm{a}}\mathbf{x}_{\mathrm{a}}^{\mathrm{T}} \right] \tag{18}$$

The covariance matrix $\mathbf{\Gamma}_{\mathbf{x}_{\mathrm{a}}}$ can be determined through [8],

$$\dot{\mathbf{\Gamma}}_{\mathbf{x}_{\mathrm{a}}} = \mathbf{A}_{\mathrm{a}}\mathbf{\Gamma}_{\mathbf{x}_{\mathrm{a}}} + \mathbf{\Gamma}_{\mathbf{x}_{\mathrm{a}}}\mathbf{A}_{\mathrm{a}}^{\mathrm{T}} + 2\pi\mathbf{B}_{\mathrm{a}}\mathbf{S}_0\mathbf{B}_{\mathrm{a}}^{\mathrm{T}} \tag{19}$$

If the excitation is stationary, the stationary solution can be obtained from the Lyapunov equation,

$$\mathbf{0} = \mathbf{A}_{\mathrm{a}}\mathbf{\Gamma}_{\mathbf{x}_{\mathrm{a}}} + \mathbf{\Gamma}_{\mathbf{x}_{\mathrm{a}}}\mathbf{A}_{\mathrm{a}}^{\mathrm{T}} + 2\pi\mathbf{B}_{\mathrm{a}}\mathbf{S}_0\mathbf{B}_{\mathrm{a}}^{\mathrm{T}} \tag{20}$$

Because the state matrix $\mathbf{A}_{\mathrm{a}}$ is a function of $\mathbf{C}_{\mathrm{eq}}$ and $\mathbf{K}_{\mathrm{eq}}$, which are also functions of the response, Eq. (20) should be iteratively determined [15]. To start the iteration, a corresponding linear system with initial parameters of the nonlinear system is applied to get initial $\mathbf{C}_{\mathrm{eq},0}$ and $\mathbf{K}_{\mathrm{eq},0}$ [16].

The covariance matrix of output structural responses, $\mathbf{\Gamma}_{\mathbf{y}}$, is given by

$$\mathbf{\Gamma}_{\mathbf{y}_{\mathrm{s}}} = \mathbf{C}_{\mathrm{a}}\mathbf{\Gamma}_{\mathbf{x}_{\mathrm{a}}}\mathbf{C}_{\mathrm{a}}^{\mathrm{T}} \tag{21}$$

2.4 Structural optimization formulation

The formulation of the BRBF optimization problem in this paper is given by

$$\begin{aligned} &\text{Find the design variables: } \boldsymbol{\theta} = \left\{ \theta_1 \quad \theta_2 \quad \dots \quad \theta_n \right\}^{\mathrm{T}} \in \mathrm{R}^{\mathrm{n}} \\ &\text{Minimize: } J\left(\boldsymbol{\theta}\right) = \mathrm{E}\left[\mathbf{y}_{\mathrm{s}}^{\mathrm{T}} \mathbf{Q} \mathbf{y}_{\mathrm{s}} \right] \\ &\text{Subject to: } \begin{cases} \theta_{j,\min} < \theta_j < \theta_{j,\max}, & j = 1, 2, ..., n \\ \mathrm{E}\left[G_k(\mathbf{y}_{\mathrm{s}}, \boldsymbol{\theta}) \right] \le 0, & k = 1, 2, ..., m \end{cases} \end{aligned} \tag{22}$$

where θ_j represents the j^{th} design variable, $\boldsymbol{\theta}$ represents the design variables vector. In this study, the design variables are chosen to be the lateral stiffness of the BRBs. $J\left(\boldsymbol{\theta}\right)$ is the objective function to be minimized, which refers to the stationary structural responses. $\theta_{j,\min}$ and $\theta_{j,\max}$ represent the lower and upper bound of the j^{th} design variable respectively. $G_k(\mathbf{y}_{\mathrm{s}}, \boldsymbol{\theta})$ represents the k^{th} constraint function in the optimization procedure. $\mathbf{Q}$ is a positive definite matrix expressing the relative importance of the output responses in $\mathbf{y}_{\mathrm{s}}$. The stationary responses are calculated as

$$\mathrm{E}\left[\mathbf{y}_{\mathrm{s}}^{\mathrm{T}} \mathbf{Q} \mathbf{y}_{\mathrm{s}} \right] = \mathrm{E}\left[\mathbf{x}_{\mathrm{a}}^{\mathrm{T}} \mathbf{C}_{\mathrm{a}}^{\mathrm{T}} \mathbf{Q} \mathbf{C}_{\mathrm{a}} \mathbf{x}_{\mathrm{a}} \right] = \mathrm{trace}\left[\mathbf{C}_{\mathrm{a}}^{\mathrm{T}} \mathbf{Q} \mathbf{C}_{\mathrm{a}} \boldsymbol{\Gamma}_{\mathbf{x}_{\mathrm{a}}} \right] \tag{23}$$

where the covariance of the augmented system responses $\boldsymbol{\Gamma}_{\mathbf{x}_{\mathrm{a}}}$ is given by the solution of Eq. (20).

Because the BRBF optimization is a non-convex problem, the gradient-based algorithms always encounter local minimum and fail to obtain the global optimum designs. Therefore, the generalized pattern search (GPS) algorithm is employed to perform the optimization procedure, as it does not require gradient information to direct the optimization [17]. The algorithm consists of an exploratory move, followed by a pattern move [18]. The exploratory search starts by evaluating the objective function at the initial design $\boldsymbol{\theta}_0$, i.e., $J\left(\boldsymbol{\theta}_0\right)$, and aims to obtain the optimization direction for the following pattern move [19]. Design variables in the vector $\boldsymbol{\theta}$ are updated individually with the same step size. When no such increase or decrease in any one parameter further reduces the objective function $J\left(\boldsymbol{\theta}_0\right)$, the steps are halved in size. The process is repeated until the steps are less than the convergence tolerance, at which point the optimal value of the parameter vector, $\boldsymbol{\theta}_{\text{opt}}$, is obtained.

3. BRBF optimization

This paper optimizes the BRBF system of a full-scale five-story steel frame structure to illustrate the proposed procedure and validate the efficacy of the approach. The BRBF is seismically excited and constructed with two BRBFs in each direction, and each BRBF consists of two BRBs in each floor, as shown in Fig. 1. Each BRBF is assumed to resist half of the seismic load in each direction. For simplification, the two BRBs in each BRBF are assumed to have the same design. The illustrative example was initially designed by Bruneau et al. [20] applying the equivalent lateral force (ELF) procedure as specified by ASCE-7.

This study takes a single plane BRBF as the example and idealizes it as a shear beam model. The typical BRBF in the five-story steel frame is three-bay, with 6.096m longitudinal span. The typical story height is 3.9624m and the first story height is 5.4864m. The typical story mass for each BRBF is 1.05×10^6 kg and the first story mass is 1.12×10^6 kg. The detailed beam, column and connection information are described by Bruneau et al. [20]. The damping ratio for each modes is assumed to be 5%. The damping matrix $\mathbf{C}$ is calculated assuming modal damping. The natural frequencies are 0.94, 2.37, 3.70, 4.91 and 6.34 Hz. Note that the angle between the BRBs and the floors should be taken into consideration in the calculation of the BRBs stiffness.

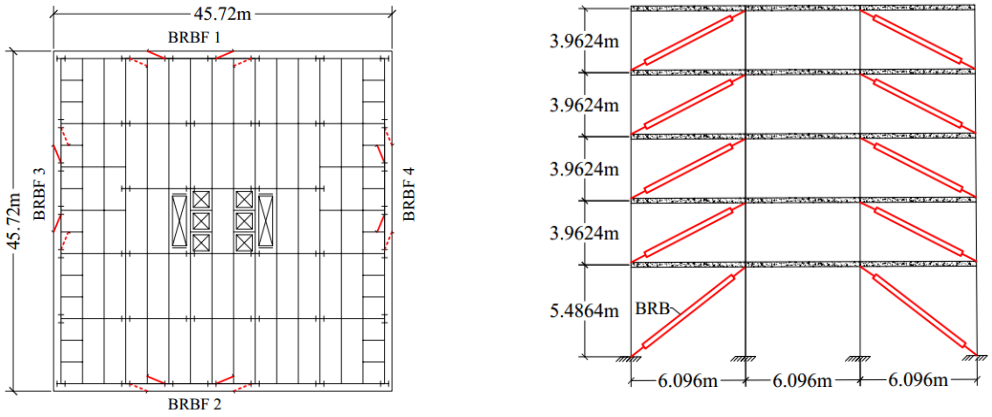

(a) Typical floor plan (b) Typical frame elevation

Fig. 1 – Schematic diagram of the illustrative example

3.1 Optimized stiffness distribution

The stiffness of the BRBs on each floor is determined as the design variables, i.e., $\boldsymbol{\theta}=[k_{\mathrm{b1}} \quad k_{\mathrm{b2}} \quad \ldots \quad k_{\mathrm{b5}}]^{\mathrm{T}}$. In this paper, the BRBF is optimized from two initial conditions to ensure the robustness of the proposed procedure. The first initial design is obtained from Bruneau et al. [20] according to the ELF procedure, referred as "initial design (ELF)" in the following sections. The other initial design is obtained by a more convenient method, which designs only the BRB stiffness of the first floor and distributes the same design along all the upper stories. The second initial condition is referred as "initial design (uniform)" as follows.

The design domain should be around the reasonable initial design. Therefore, the lower and upper bound of each design variable are set to be one tenth and tenfold respectively, i.e., $\theta_{j,\min}=1/10\theta_{0,j}$, $\theta_{j,\max}=10\theta_{0,j}$. The sum of structural stiffness is constrained to be less than or equal to the sum of the initial stiffness, i.e.,

$$G_1(\boldsymbol{\theta})=\sum k_{\mathrm{bj}}-\sum k_{\mathrm{bj},0} \tag{24}$$

Assuming the BRBs in each story are equally significant, then the positive definite matrix $\mathbf{Q}$ in the objective function is a unity matrix (i.e., $\mathbf{Q}=\mathbf{I}_5$). This study employs interstory drift ratio ($J_1(\boldsymbol{\theta})$) and the ductility demand ($J_2(\boldsymbol{\theta})$) as the objectives. The interstory drift ratio is considered to be an indicator of structural safety. Ductility is a measure used in practice to describe the plastic demand of a BRB device. The ductility demand is formulated as

$$\mu_j=\frac{u_{l,j}}{u_y}=\frac{d_j}{u_{\mathrm{y}}}\frac{\sqrt{H_j^2+S_j^2}}{H_j} \tag{25}$$

where μ_j is the ductility demand; $u_{l,j}$ is the displacement in the axial direction of a BRB; d_j is the interstory drift of the j^{th} floor. H_j, S_j are the story height and span length of the specified story. The ductility demand considers not only the interstory drift, but also the influence of story height and span length.

For comparison purposes, this example considers the same seismic hazard conditions as presented by Bruneau et al. [20], which is for a moderate to high seismicity area with D site classification, $S_{\mathrm{DS}}=0.733\mathrm{g}$ and $R=8$. Because the peak ground acceleration (PGA) is commonly 3□4 times the root mean square (RMS) absolute ground acceleration [21], in this paper, the RMS ground acceleration of the design high intensity earthquake is determined to be $a_{\mathrm{g}}=S_{\mathrm{DS}}/4R\approx 0.224\mathrm{m/s}^2$. Correspondingly, $S_0=4.5873\times10^{-4}$. The excitation is modeled as the mean-value KT spectrum, with $\omega_g=20.3\mathrm{rad/sec}$ and $\zeta_g=0.32$ [22].

This study employs the unbonded BRBs in the structural design. An unbonded BRB consists of four parts: inner core, outer tube, encasing mortar, and debonding material, as shown in Fig. 2. The inner core section and outer tube are commonly made of steel, with Young's modulus of $E = 200\text{GPa}$. The encasing mortar and debonding material are infilled between the inner core and outer tube. The inner core is connected with the basic structural framework and is mainly responsible of sustaining axial loads. The outer tube and encasing mortar prevent the inner core from buckling. The debonding material provides a smooth surface for the inner core to slip freely along the encasing mortar to dissipate seismic energy [4]. A single BRB has three cross sections along its inner core: a yielding section in the middle, and two connection sections at both ends. The yielding section is to dissipate energy during seismic excitation, and the connection sections has gradually increased cross-section areas to concentrate all the inelastic activity at the yielding section. By conducting pseudo-static cyclic tests and model parameter estimation, Black et al. [4] proposed a parameter set for a nominal unbonded BRB, i.e., $\gamma = 0.45$, $\beta = 0.55$, $A = 1$, $\alpha = 0.025$, $n = 1$ and $u_y = 6.04\text{mm}$. This study applies this typical parameter set to represent the hysteretic behavior of the BRBs.

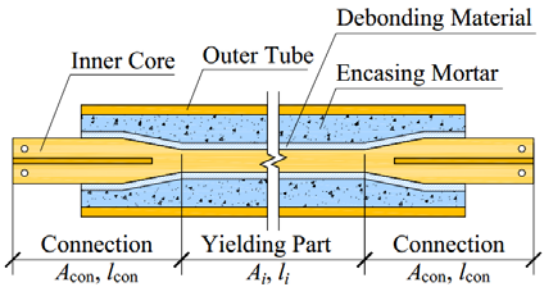

Fig. 2 – Schematic diagram of an unbonded BRB

The optimal stiffness distribution of the BRBs corresponding to the initial design (ELF) are shown in Table 1 and graphically depicted in Fig.3a. The optimized results of the initial design (uniform) are shown in Table 2 and Fig. 3b. Despite the different initial stiffness, the stiffness distribution tendency of both optimized designs are the same. In both cases, to minimize the interstory drift ratio response, the structure tends to distribute the stiffness non-uniformly along story height, with more stiffness assigned to the second floor. The stiffness distribution minimizing ductility response (red line in corresponding figures) is inversely proportional with story height and more stiffness is distributed at the first floor due to the higher story height. Note that the initial design (ELF) is similar with the optimized design minimizing the interstory drift ratio.

Table 1 – Optimized BRB stiffness with initial design (ELF) (10^6 N/m)

Story	**1st**	**2nd**	**3rd**	**4th**	**5th**
Initial design (ELF)	232.2	243.6	200.5	142.9	91.8
$J_1(\boldsymbol{\theta})$	227.7	245.4	204.7	151.5	81.8
$J_2(\boldsymbol{\theta})$	305.6	211.2	182.6	136.9	74.6

Table 2 – Optimized BRB stiffness with initial design (uniform) (10^6 N/m)

Story	**1st**	**2nd**	**3rd**	**4th**	**5th**
Initial design (uniform)	232.2	232.2	232.2	232.2	232.2
$J_1(\boldsymbol{\theta})$	389.7	269.2	232.7	174.5	95.0
$J_2(\boldsymbol{\theta})$	290.3	312.6	260.9	193.1	104.2

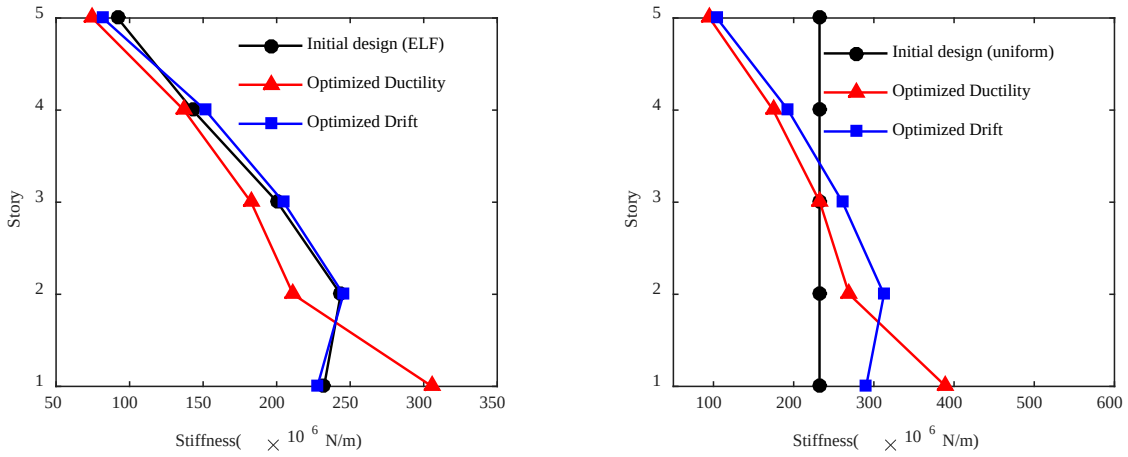

(a) Initial design (ELF) (b) Initial design (uniform)

Fig. 3 – Optimized stiffness distribution of the BRBs with different initial designs

3.2 Structural responses

The interstory drift and ductility responses of the optimized designs with initial design (ELF) are shown in Fig. 4. The interstory drift ratio of the design minimizing $J_1(\boldsymbol{\theta})$ (blue line in Fig. 4a) is the same along each floor, while the ductility of the first floor is much larger than other floors (blue line in Fig. 4b). This ductility distribution indicates that more energy is dissipated at the bottom floor and the yielding of the BRBs at the first floor is more severe than the other stories. This "soft-first-story" building is not safe subjected to high-intensity earthquake. The design minimizing ductility responses obtains the same ductility responses in each story (red line in Fig. 4b), while the interstory drift ratio of the first floor is much smaller than other stories (red line in Fig. 4a). The pattern is the same in the optimal designs with initial design (uniform), as shown in Fig. 5.

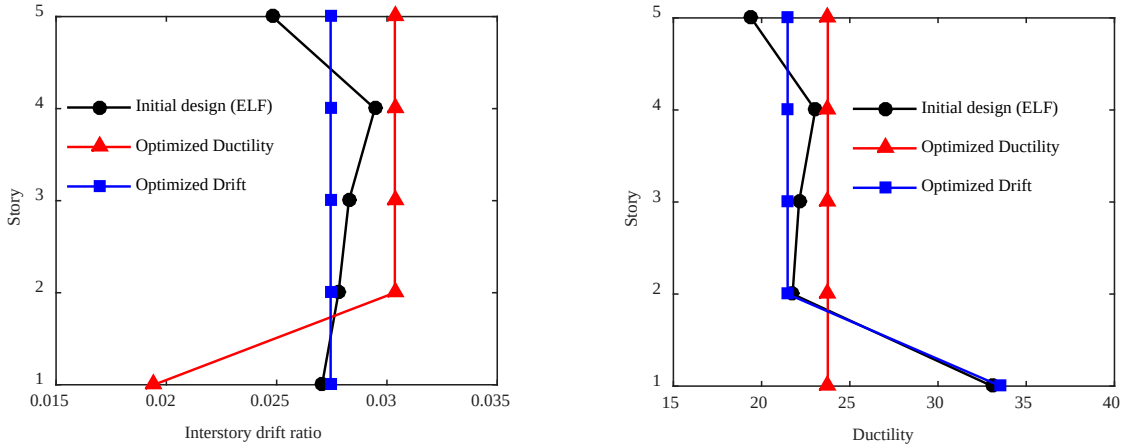

(a) Interstory drift ratio (b) Ductility

Fig. 4 – Structural responses of optimal results with initial design (ELF)

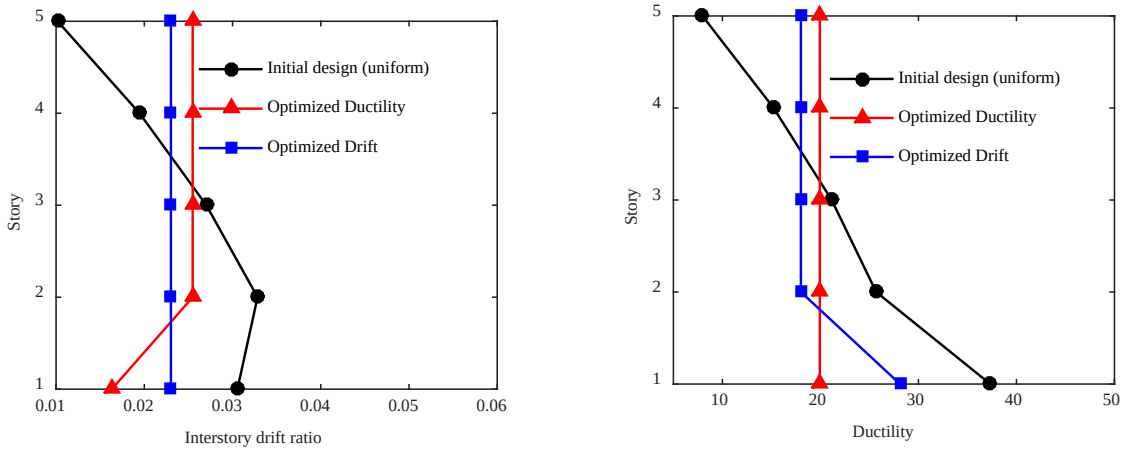

(a) Interstory drift ratio (b) Ductility

Fig. 5 – Structural responses of optimal results with initial design (uniform)

3.3 Maximum BRB stiffness design

Note that in Fig. 5b, with uniform stiffness distribution, ductility responses are inversely proportional to the story height (black line in Fig. 5b), hence the energy dissipation decreases along the story height. In high-rise structures with uniformly distributed stiffness, the higher stories will dissipate less energy. The stories with $\mu \le 1$ remain linearly elastic during high intensity earthquake and the over-sized BRBs are not capable of energy dissipation. This convenient uniform design tends to over design the BRBs of the higher stories.

To ensure the seismic energy dissipation, the maximum BRB stiffness should be determined by ductility requirements. Because a BRB with ductility ratio $\mu \le 1$ remains elastic and does not dissipate seismic energy, the upper bound of a BRB stiffness design is to activate the constraint $\mu = 1$. The maximum BRB stiffness of the ELF design is shown in Fig. 6. With the initial design based on the ELF procedure, the maximum BRB stiffnesses are $\left[2.51 \quad 1.73 \quad 1.50 \quad 1.13 \quad 0.62\right]^{\mathrm{T}} \times 10^{10}$ N/m. The optimized designs with both initial conditions are less than the maximum bound.

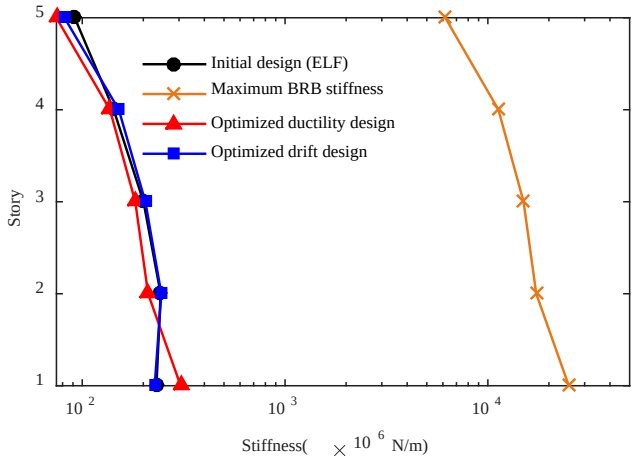

Fig. 6 – Maximum BRB stiffness with initial design (ELF)

4. Conclusion

This study proposes a procedure for the BRBF structural optimization under seismic excitation. The procedure optimizes the stiffness distribution of the BRBs at the system-level and designs the BRBs according to the

obtained optimum stiffness at the component-level. A zero-mean filtered white noise is employed to represent the seismic excitation and both the structure and the shaping filter are combined to formulate the augmented system. The proposed approach incorporates the stochastic nature of seismic dynamic loading directly in the optimization process. To demonstrate the efficacy of the proposed approach, a five-story BRBF subjected to random seismic excitation is optimized. The hysteretic behavior of the BRBs is modeled by the Bouc-Wen model. Analysis is done via stochastic equivalent linearization. The minimization of both the interstory drift ratio and ductility are discussed in this paper. Optimization is conducted with different initial design to assess robustness of the proposed procedure. The optimization results are compared with the common design specified by the ASCE-7 and the simplified design of uniformly distributed BRB stiffness.

The proposed procedure distributes the stiffness along the story height non-uniformly to minimize the interstory drift ratio response, which is similar with the initial design according to the ELF procedure. The interstory drift ratio in each floor of this design is the same and the maximum value is minimized. However, the ductility of the first floor is much larger than other floors, which may increase the vulnerability of structural system. The design objective of minimizing maximum ductility response tends to distribute stiffness almost linearly, and inversely proportional to the story height. The BRB ductility of each floor in this design is the same, which guarantees that the seismic energy is evenly dissipated along the structure height. To ensure the effective energy dissipation, the stiffness of the BRBs should be less than the maximum design stiffness, with which design the ductility is equal to unity.

In summary, the minimized and uniformly distributed ductility should be considered as the optimization objective in the BRBF design instead of the minimization of the interstory drift. Future studies will assess the effects of structural height and vertical geometric irregularity in the optimal design.

5. Acknowledgements

The first author gratefully acknowledges the support of the China Scholarship Council to the University of Illinois at Urbana-Champaign. The second author gratefully acknowledges the financial support of CONICYT-Chile through the Becas Chile Scholarship, and Federico Santa Maria Technical University (UTFSM) through the Faculty Development Program Scholarship.

6. References

[1] Skinner, R. I., Kelly, J. M., & Heine, A. J. (1975): Hysteretic dampers for earthquake-resistant structures. *Earthquake Engineering & Structural Dynamics*, **3** (3), 287-296.

[2] Lin, P. C., Tsai, K. C., Wu, A. C., Chuang, M. C., Li, C. H., & Wang, K. J. (2015): Seismic design and experiment of single and coupled corner gusset connections in a full-scale two-story buckling-restrained braced frame. *Earthquake Engineering & Structural Dynamics*, **44** (13), 2177-2198.

[3] Sarno, L. Di, & Elnashai, A. S. (2005): Innovative strategies for seismic retrofitting of steel and composite structures. *Earthquake Engineering & Structural Dynamics*, **7** (3), 115-135.

[4] Black, C. J., Makris, N., & Aiken, I. D. (2004): Component testing, seismic evaluation and characterization of buckling-restrained braces. *Journal of Structural Engineering*, **130** (6), 880-894.

[5] Fahnestock, L. A., Ricles, J. M., & Sause, R. (2007): Experimental evaluation of a large-scale buckling-restrained braced frame. *Journal of Structural Engineering*, **133** (9), 1205-1214.

[6] Fahnestock, L. A., Sause, R., & Ricles, J. M. (2007): Seismic response and performance of buckling-restrained braced frames. *Journal of Structural Engineering*, **133** (9), 1195-1204.

[7] Balling, R. J., Balling, L. J., & Richards, P. W. (2009): Design of buckling-restrained braced frames using nonlinear time history analysis and optimization. *Journal of Structural Engineering*, **135** (5), 461-468.

[8] Soong, T. T., & Grigoriu, M. (1993): *Random Vibration of Mechanical and Structural Systems*. Prentice Hall.

[9] Farhat, F., Nakamura, S., & Takahashi, K. (2009): Application of genetic algorithm to optimization of buckling restrained braces for seismic upgrading of existing structures. *Computers and Structures*, **87** (1), 110-119.

[10] Wen, Y.K. (1976): Method for random vibration of hysteretic systems. *Journal of the Engineering Mechanics Division*, **102** (2), 249-263.

[11] Spencer Jr., B. F., & Bergman, L. A. (1985): On the reliability of a simple hysteretic system. *Journal of Engineering Mechanics*, **111** (12), 1502-1514.

[12] Wen, Y.K. (1980): Equivalent linearization for hysteretic systems under random excitation. *Journal of Applied Mechanics*, **47** (1), 150-154.

[13] Kanai, K. (1957): Semi-empirical formula for the seismic characteristics of the ground. *Earthquake Research Institute*, University of Tokyo.

[14] Tajimi, H. (1960): A statistical method for determining the maximum response of a building structure during an earthquake. *In Proc. of the 2nd WCEE*, **2**, 781-797.

[15] Bingqi, M. (1993): Direct integration variance prediction of random response of nonlinear systems. *Computers & Structures*, **46** (6), 979-983.

[16] Hurtado, J. E., & Barbat, A. H. (2000): Equivalent linearization of the Bouc-Wen hysteretic model. *Engineering Structures*, **22** (9), 1121-1132.

[17] Kolda, T. G., Lewis, R. M., & Torczon, V. (2003): Optimization by direct search: new perspectives on some classical and modern methods. *SIAM Review*, **45** (3), 385-482.

[18] Hooke, R., & Jeeves, T. A. (1961): "Direct search" solution of numerical and statistical problems. *Journal of the ACM (JACM)*, **8** (2), 212-229.

[19] Rios, L. M., & Sahinidis, N. V. (2013): Derivative-free optimization: a review of algorithms and comparison of software implementations. *Journal of Global Optimization*, **56** (3), 1247-1293.

[20] Bruneau, M., Uang, C., & Sabelli, S. (2011): *Ductile Design of Steel Structures*. McGraw Hill Professional.

[21] Boggs, D. (1997): Acceleration indexes for human comfort in tall buildings-Peak or RMS. *In CTBUH Monograph*, 1-21.

[22] Lai, S.-S. P. (1982): Statistical characterization of strong ground motions using power spectral density function. *Bulletin of the Seismological Society of America*, **72** (1), 259-274.